

CONCREEP 10

*Mechanics and Physics of Creep,
Shrinkage, and Durability of Concrete and
Concrete Structures*

PROCEEDINGS OF THE 10TH INTERNATIONAL CONFERENCE
ON MECHANICS AND PHYSICS OF CREEP, SHRINKAGE, AND
DURABILITY OF CONCRETE AND CONCRETE STRUCTURES

September 21-23, 2015
Vienna, Austria

SPONSORED BY
RILEM
Engineering Mechanics Institute of ASCE

EDITED BY
Christian Hellmich
Bernhard Pichler
Johann Kollegger



Published by the American Society of Civil Engineers

Computational Fatigue Life Assessment of Corroded Reinforced Concrete Beams

Y. Tanaka¹; Y. Takahashi²; and K. Maekawa³

¹Department of Human and Social Systems, Institute of Industrial Science, The University of Tokyo, 4-6-1, Komaba, Meguro-ku, Tokyo 153-8505. E-mail: yasuxi@iis.u-tokyo.ac.jp

²Concrete Laboratory, Department of Civil Engineering, The University of Tokyo, 7-3-1, Hongo, Bunkyo-ku, Tokyo 113-8656. E-mail: takahashi@concrete.t.u-tokyo.ac.jp

³Concrete Laboratory, Department of Civil Engineering, The University of Tokyo, 7-3-1, Hongo, Bunkyo-ku, Tokyo 113-8656. E-mail: maekawa@concrete.t.u-tokyo.ac.jp

Abstract

Remaining performance of corroded reinforced concrete beams is numerically evaluated by means of poro-mechanics approach. Corrosion substance is treated as the combined phases of liquid and solid gels. The static loading experiment of corroded reinforced concrete beams is fairly simulated by the multi-directional fixed crack model combined with corrosion gel migration. Further, fatigue life of corroded reinforced concrete beams is studied numerically. Even if static shear strength is not reduced so much, remaining fatigue life could be shortened significantly due to the cyclic degradation of cracked cover concrete around expanded steel bars.

INTRODUCTION

Aged bridges in service of more than 50 years are increasing over the world and many of them are deteriorated due to steel corrosion located close to the sea shores. For maintaining these infrastructures as a social asset, quantitative assessment of life-extending effect by repair work is crucial. Not only the static capacity for safety performance but also the service-life related to fatigue shall be encompassed in maintenance planning. In this study, the coupled issue of steel corrosion and mechanistic fatigue loads are discussed as an engineering target. RC beams and decks of which bridges consist are subjected to high cycle repetition of dynamic loads. Herein, it is of great importance to estimate the remaining service-life. This study aims at corroded RC beams and guarders under fatigue actions by simulating steel corrosion with poro-mechanics approach.

NUMERICAL MODELING

Remaining fatigue life is assessed by multi-scale chemo-physical simulation in this study. Logarithmic-integral scheme (Maekawa and Fujiyama, 2013a) is

applied in case where compression, shear and tensile fatigue models are combined into the multi-directional fixed crack model (Maekawa et al. 2003) as summarized in Figure 1. Time-dependent deformation is also considered by the evolution law of the damage parameter K_c .

	Compression	Tension	Shear transfer
Core Constitutive Laws	<p>Stress – Strain</p> <p>$\sigma = E_0 K_c \epsilon_e$ $\epsilon = \epsilon_e + \epsilon_p$</p> <p>Maekawa et al. 2003⁶</p>	<p>Stress – Strain</p> <p>$\sigma = E_0 K_t \epsilon_e$ $\epsilon = \epsilon_e + \epsilon_p$</p> <p>Maekawa et al. 2003⁶</p>	<p>Shear stress - Slip or Strain</p> <p>$\tau = \int_{-\tau/2}^{\tau/2} R'(\omega, \delta, \theta) \sin \alpha \theta d\theta$</p> <p>Maekawa et al. 2003⁶</p>
Enhanced model for High cycle Fatigue	<p>Fracture parameter K_c considers time dependent plasticity & fracturing and cyclic fatigue damage</p> $dK_c = \left(\frac{\partial K_c}{\partial t} \right) dt + \left(\frac{\partial K_c}{\partial \epsilon_e} \right) d\epsilon_e$ <p>Time dependency Cyclic fatigue</p> <p>$\left(\frac{\partial K_c}{\partial \epsilon_e} \right) = \lambda \sim \text{when } F_k = 0$ $\left(\frac{\partial K_c}{\partial \epsilon_e} \right) = - \left(\frac{\partial F_k}{\partial \epsilon_e} \right) \left(\frac{\partial F_k}{\partial K} \right) + \lambda \sim \text{when } F_k = 0$ $\lambda = K^3 \cdot (1 - K^4) \cdot g \cdot R$ El-Kashif and Maekawa 2004¹⁰</p>	<p>Fracture parameter K_T considers time dependent fracturing and cyclic fatigue damage</p> $dK_T = F dt + G d\epsilon_e + H d\epsilon_s$ <p>Time dependent fracturing Cyclic fatigue damage</p> <p>Maekawa et al. 2003⁶, Hisasue 2005¹⁴</p>	<p>Accumulated path function X reduce shear associated with cyclic fatigue damage</p> $\tau = X \cdot \tau_0(\delta, \omega)$ <p>function original model</p> $X = 1 - \frac{1}{10} \log_{10} \left(1 + \int d(\delta/\omega) \right) \geq 0.1$ <p>Contact density model by Li & Maekawa 1989¹⁵, Modification of accumulated path function by Gebreyouhannes 2006¹⁶</p>
Physical meaning	Decrease of stiffness and plasticity accumulation by continuous fracturing concrete	Decrease of tension stiffness by bond fatigue	Decrease of shear transfer normal to crack by continuous deterioration of rough crack surface

Figure 1. Constitutive laws for high cycle fatigue (Maekawa et al. 2003)

The authors pay their attention to the location of corrosion and the deteriorated bond through the cracked cover concrete. Here, poro-mechanics modeling (Maekawa and Fujiyama, 2013b) of corrosion gel substances is coupled with solid skeleton based on Biot’s theory. Original governing equation for isotropic soil-pore system is described as follows.

$$\sigma_{ij} = \sigma_{ij}^* + \delta_{ij} p \tag{1}$$

where, σ_{ij} is total stress, σ_{ij}^* is effective stress and p is pore pressure. Effective stress of skelton phase is calculated from the constitutive laws as shown in Figure 1, while the substantial linear stiffness is assumed for pore pressure as,

$$p = \overline{K_f} (w_{ii} + \epsilon_{ii}) \tag{2}$$

$$\overline{K_f} = \left(\frac{1-n}{K_c} + \frac{n}{K_g} \right)$$

where, K_c and K_g are bulk stiffness of concrete matrix and corrosion gel, $w_{ii} + \epsilon_{ii}$ is volumetric strain of corrosion gel inside cracked concrete and n is constant to represent the effect of porosity. As to volumetric strain of corrosion gel, volumetric expansion ratio of corrosion substances is assumed as 5.0. While this two phase model was originally developed for concrete-pure water interaction, corrosion gel is the mixture of liquid and solid. Therefore, part of corrosion product is assumed as

crystalline solid, while the rest is assumed as liquid. Ratio of the crystalline phase is simply assumed to be 30 % in this study. The Darcy law is used to consider the flow of liquid phase of the corrosion gels. The permeability of corrosion gel in capillary pores κ^* is assumed as 10^{-12} m/s, which is significantly smaller than that of pure condensed water (10^{-7} m/s).

In cracked concrete, the authors apply anisotropy by assuming that pore water pressure acts perpendicular to the crack plane as,

$$\sigma_{ij} = \sigma_{ij}^* + \delta_{ij} l_i p \tag{3}$$

where, l_i is the unit directional vector normal to crack plane (Figure 2). The permeability of cracked concrete is estimated as a function of crack width.

$$\kappa_i = \kappa^* \left\{ 1 + \left(\frac{\varepsilon_{jj} + \varepsilon_{kk}}{a} \right)^4 \right\} \tag{4}$$

$\varepsilon_{jj} + \varepsilon_{kk}$ is the transverse in-plane strain. a is material constant where $1.0E^{-4}$ is assumed tentatively.

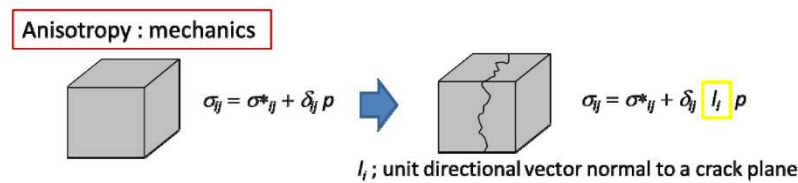


Figure 2. Anisotropy of cracked concrete

BOND DEGRADATION IN STATIC BEAM TEST

The flexural-shear experiment of RC beams with corrosion along longitudinal bars (Kanaduka *et al.* 2011) is simulated numerically. Figure 3 shows the dimensions of the targeted beam specimens. Cover depth, which is the main parameter in this experimental series, is 40 mm (C40) or 60 mm (C60). Entire length of the longitudinal bars was forced to be corroded electrochemically until the cross sectional area was reduced by 8 % on average. The compressive strength of concrete is $33N/mm^2$. The high-strength reinforcing bars, which yield strength is $750N/mm^2$, are used not to fail in flexure.

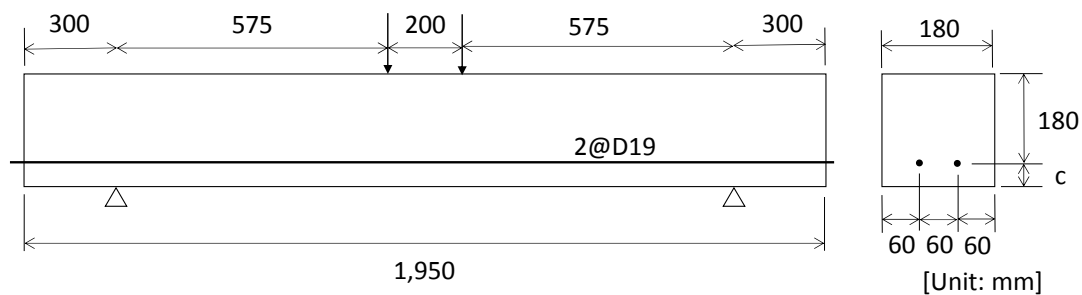


Figure 3. Dimensions of beam specimen (Kanaduka *et al.* 2011)

After the accelerated corrosion experiment, those simply supported beams were loaded concentrically. The shear span to effective depth ratio (a/d) is 3.19 while the development length is selected as 300 mm (15.8D).

As shown in Figure 4, corrosion cracks were induced along the reinforcing bars. In the case of 60 mm of the concrete cover depth (C60), corrosion cracks appeared on both sides of the beam and the bottom face. On the contrary, corrosion cracks were observed only on the bottom face in the case of 40 mm (C40). In loading, few flexural cracks were observed due to the reduction of macroscopic bond strength associated with cracked damage of cover concrete. The diagonal crack was formed near by the loading points and it propagated along with the longitudinal bars. Failure occurred when a diagonal shear crack reached the end of specimen.

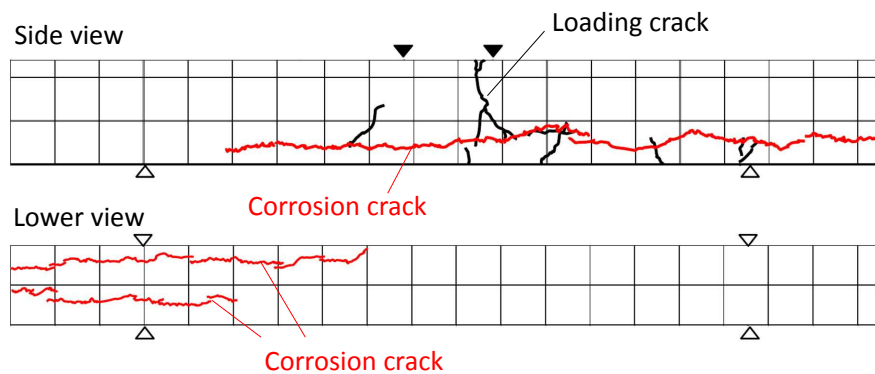
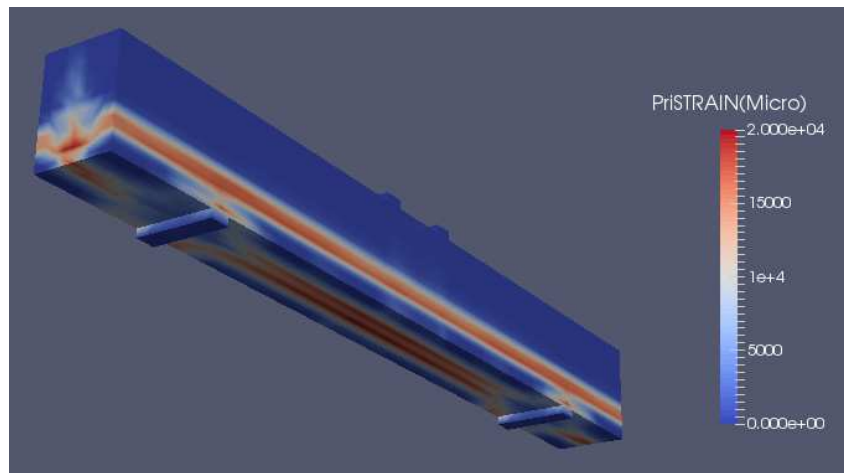
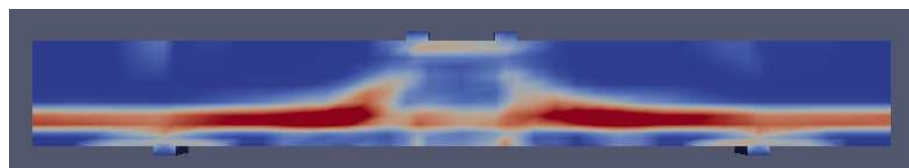


Figure 4. Crack patterns observed in experiment (C60)



(a) Corrosion cracks before the loading (Bottom perspective view)



(b) After loading (Side view)

Figure 5. Post-loading crack patterns estimated by the analysis (C60)

Figure 5 shows estimated cracks before and after the loading. It is obvious that numerical simulation may capture both corrosion crack before loading and those induced by the external loading. Diagonal crack formed near loading plate and its propagation caused failure. Figure 6 shows the load - deflection relations of analyzed specimens. Numerical simulation is able to estimate lower loading capacity of C40 specimen which has smaller cover depth. This is because resultant restriction force of cracked cover concrete is naturally calculated by applying the chemo-mechanics model. Otherwise, we need to set up bond-slip model between reinforcement and concrete by considering corrosion cracks, cover concrete, envelop re-bars and so on. In many cases, the bond strength and bond-slip relations are not material properties but the resultant of the mechanistic damage of the beam. Then, the apparent bond-slip relation is not unique but different according to the damage patterns of cover concrete and their location. The bond deterioration is not the unique characteristics but to be computed value.

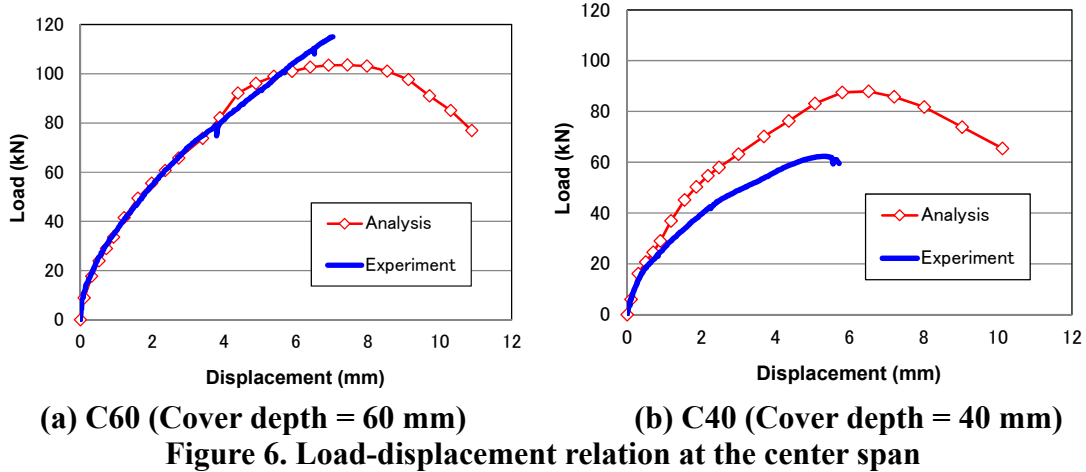


Figure 6. Load-displacement relation at the center span

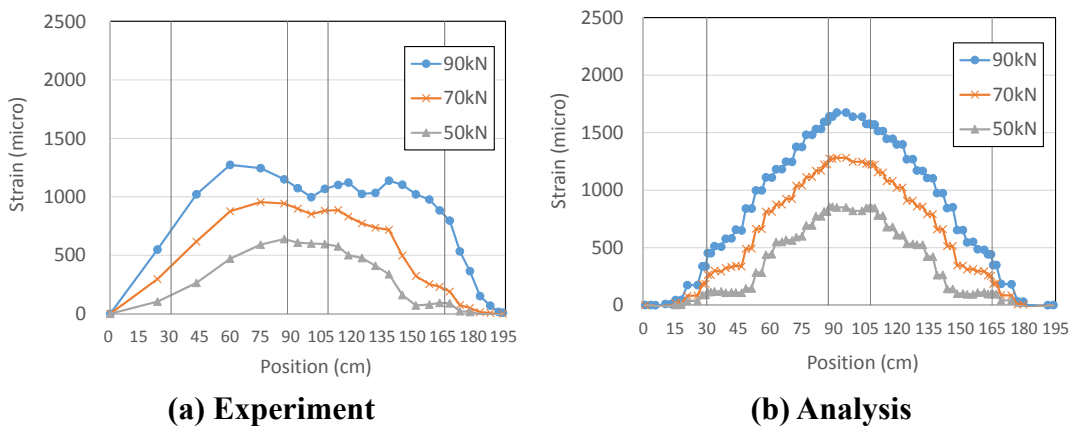


Figure 7. Steel strain distribution along the beam axis (C60)

Figure 7 shows the steel strain distribution along the main reinforcement in several load levels. In experiment, steel strain is constant beyond constant moment span due to the weakened bond strength. Pretty high steel strain is observed at

supporting point as the load increases. Even though the numerical analysis simulates developed strain profile in anchorage, smaller de-bonding effect is expected compared with experiment. Within the constant moment span, constant strain is calculated in lower load such as 50kN. In contrast, inclined strain profile is achieved in higher load level (70kN and 90 kN) because damages are induced asymmetrically. Figure 8 shows numerical result of steel strain distribution in case the amount of corrosion substance increases double. Increase of corrosion product results in the higher steel strain distribution. Because steel strain profile is somewhat different from that of experiment, there is a room for improvement of our model.

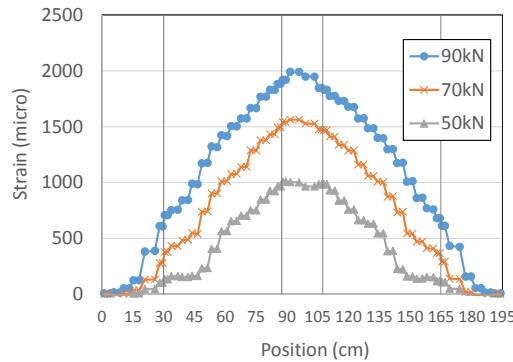


Figure 8. Numerical result of steel strain distribution in case of 16 % of weight loss due to corrosion

FATIGUE ANALYSIS

Sensitivity analysis is carried out regarding fatigue strength of corroded reinforcing beam. In this study, direct pass integral scheme is applied to simulate the progress of fatigue damage. Figure 9 shows the numerical results of center span deflections. However static shear strength of corroded beam is barely reduced, failure cycle of fatigue load decreases significantly. Compared with sound beam, fatigue life is shortened especially in case of lower repeated load as shown in Figure 10. This is because corrosion product is weak against cyclic slip. Kuroda *et al.* (2014) and Kivell *et al.* (2014) found the bond strength of corroded reinforcing bar drops drastically under

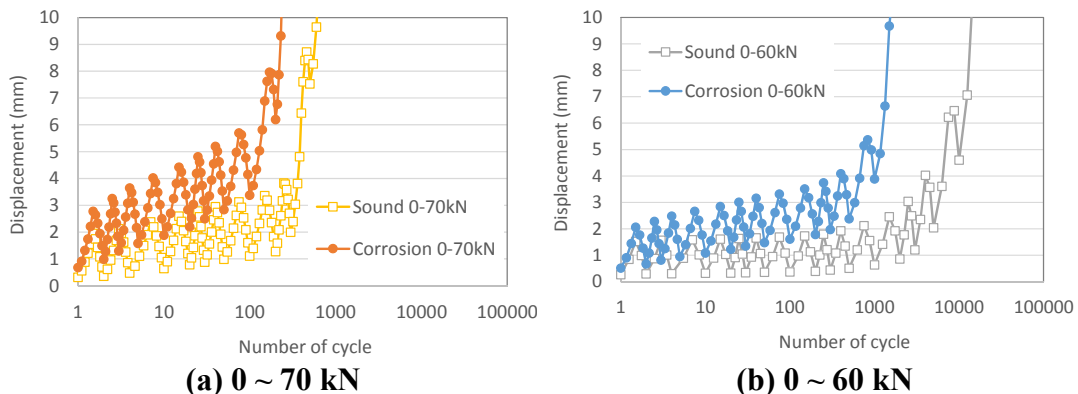


Figure 9. Progressive displacement at the span center under the high cycle repetition of loads.

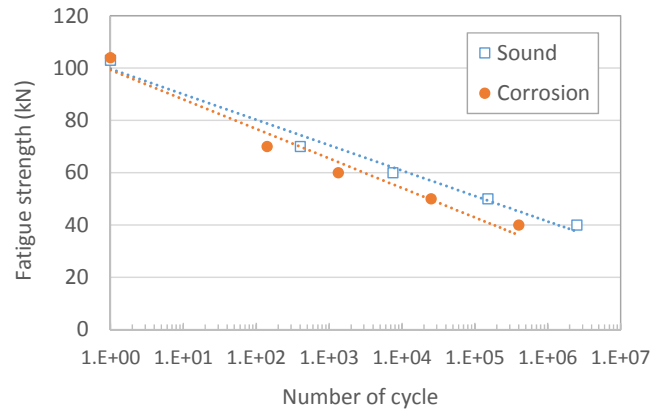


Figure 10. S – N diagram

the cyclic load in pull out test. Corrosion product easily migrates into crack under cyclic load condition. With use of poro-mechanics scheme, this phenomenon is consistently taken into account in the numerical simulation (Maeshima *et al.* 2014).

CONCLUSION

In this study, remaining performance of corroded reinforced concrete beams are numerically simulated with Poro-mechanics approach. By considering corrosion substance as the combination of liquid and solid phases, bond deterioration and remaining shear strength of corroded reinforced concrete beams are simulated successfully. Results of fatigue analysis pointed out that even if static shear strength is barely reduced, remaining fatigue life could be shortened significantly due to the degradation of bond strength under cyclic deformation.

ACKNOWLEDGEMENT

Authors appreciate Dr. Murakami who provided us the experimental data. This work was supported by Council for Science, Technology and Innovation (CSTI), Cross-ministerial Strategic Innovation Program (SIP), “Maintenance, renewal and management of infrastructure” (Funding agency: JST).

REFERENCES

- Coronelli, D. and Gambarova, P. (2004). “Structural assessment of corroded reinforced concrete beams: Modeling guidelines” *J. Structural Engineering*, 130(8), 1214-1224.
- Kallias, A. N. and Rafiq, M. I. (2010). “Finite element investigation of the structural response of corroded RC beams” *Engineering Structures*, 32(9), 2984-2994.

- Kanaduka, T., Ogawa, K. and Murakami, Y. (2011). *Proceedings of JCI*, 33(1), 833-838.
- Kivell, A., Palermo, A. and Scott, A. (2014). "Complete model of corrosion-degraded cyclic bond performance in reinforced concrete" *J. Struct. Eng.*, ASCE, 04014222-1-9.
- Kuroda, (2014). "Bond behavior of corroded re-bars under alternative loads" Proc. the 15th JSMS symposium on concrete structure, 655-660.
- Maekawa, K., Pimanmas, A. and Okamura, H. (2003). "Nonlinear mechanics of reinforced concrete" Spon press
- Maekawa, K. and Fujiyama, C. (2013a). "Crack Water Interaction and Fatigue Life Assessment of RC Bridge Decks" *Poromechanics V*, ASCE, 2280-2289.
- Maekawa, K. and Fujiyama, C. (2013b). "Rate-dependent model of structural concrete incorporating kinematics of ambient water subjected to high-cycle loads" *Engineering computations*, 30(6), 825-841
- Maeshima, T., Koda, Y., Tsuchiya, S. and Iwaki, I. (2014) "Influence of corrosion of rebars caused by chloride induced deterioration on fatigue resistance in RC road deck" *J. JSCE E2*, 70(2), 208-225.
- Tran, K. K., Nakamura, H., Kawamura, K. and Kunieda, M. (2011). "Analysis of crack propagation due to rebar corrosion using RBSM" *Cement & Concrete Composite*, 33, 906-917.